

# INFLUENCE OF GEOMETRY ON THE MEAN FLOW WITHIN URBAN STREET CANYONS – A COMPARISON OF WIND TUNNEL EXPERIMENTS AND NUMERICAL SIMULATIONS

A. KOVAR-PANSKUS<sup>1</sup>, P. LOUKA<sup>2</sup>, J.-F. SINI<sup>2</sup>, E. SAVORY<sup>3\*</sup>, M. CZECH<sup>1</sup>,  
A. ABDELQARI<sup>2</sup>, P. G. MESTAYER<sup>2</sup> and N. TOY<sup>1</sup>

<sup>1</sup> *Fluids Research Centre, School of Engineering, University of Surrey, Guildford, Surrey, U.K.*

<sup>2</sup> *Ecole Centrale de Nantes, Lab de Mecanique des Fluides, Nantes, France; <sup>3</sup> Department of Mechanical and Materials Engineering, Faculty of Engineering, University of Western Ontario, London, Ontario, Canada*

(\* author for correspondence, e-mail: esavory@eng.uwo.ca)

**Abstract.** A comparison between numerical simulations and wind tunnel modelling has been performed to examine the variation with streamwise aspect ratio (width/height, W/H) of the mean flow patterns in a street canyon. For this purpose a two-dimensional (2-D) cavity was subjected to a thick turbulent boundary layer flow perpendicular to its principal axis. Five different test cases, W/H = 0.3, 0.5, 0.7, 1.0 and 2.0, have been studied experimentally with flow measurements taken using pulsed-wire anemometry. The results show that the skimming flow regime, with a large vortex in the canyon, occurred for all the cases investigated. For the cavities with W/H  $\leq$  0.7 a weaker secondary circulation developed beneath the main vortex. The narrower the canyon, the smaller the wind speed close to the cavity ground, giving increasingly poor ventilation qualities. The corresponding numerical results were obtained with the Computational Fluid Dynamics (CFD) code CHENSI that uses the standard k- $\varepsilon$  model. The intercomparison showed good agreement in terms of the gross features of the mean flow for all the geometries examined, although some detailed differences were observed.

**Keywords:** 2-D cavity, canyon, numerical simulation, pulsed-wire-anemometry, standard k- $\varepsilon$  model, ventilation, vortex

## Nomenclature

$d$	= Displacement height (m);
H, W	= Height and width of canyon (m);
$k$	= Turbulent kinetic energy ( $\text{m}^2 \text{s}^{-2}$ );
L	= Spanwise length of canyon (m);
$Re$	= Reynolds number, $U_{ref} H/\nu$ ;
$U$	= Mean velocity in X direction ( $\text{m s}^{-1}$ );
$U_{ref}$	= Freestream velocity ( $\text{m s}^{-1}$ );
$U_*$	= Friction velocity ( $\text{m s}^{-1}$ );



*Water, Air, and Soil Pollution: Focus* **2:** 365–380, 2002.  
© 2002 Kluwer Academic Publishers. Printed in the Netherlands.

$u'$	= Streamwise turbulence intensity ( $\text{m s}^{-1}$ );
$v'$	= Lateral turbulence intensity ( $\text{m s}^{-1}$ );
$w'$	= Vertical turbulence intensity ( $\text{m s}^{-1}$ );
X, Y, Z	= Cartesian coordinates (m);
$z_o$	= Roughness length (m);
$\delta$	= Boundary layer height (m);
$\varepsilon$	= Dissipation ( $\text{m}^2 \text{s}^{-3}$ );
$\nu$	= Kinematic viscosity of air ( $\text{m}^2 \text{s}^{-1}$ ).

## 1. Introduction

Many different aspects of the wind flow within urban street canyons have been studied over the past few decades, including the influence of the flow pattern on the local pollutant transport. There have been many full-scale studies, such as DePaul and Sheih (1986), which have provided descriptions of the canyon mean flow recirculation pattern. These investigations, with aspect ratios (Width (W)/Height (H)) of 0.5 to 1, showed that the main vortex shifts upwards within the canyon with decreasing canyon width (DePaul and Sheih, 1986). This also yields much higher pollutant concentrations in a canyon with W/H = 0.5 in comparison to W/H = 1 (Pavageau *et al.*, 1996). For canyons with W/H = 1, the wind speed at the roof level was found to scale linearly with the strength of the vortex flow (Nakamura and Oke, 1988). Further wind tunnel studies have investigated the influence of roof shape on the distribution of pollutants within the canyon (Rafailidis, 1997; Kastner-Klein and Plate, 1999). Liedtke *et al.* (1999) studied the influence on pollutant dispersion of the geometrical resolution of the wind tunnel model used and found distinct differences in comparison to the modelled field site study of Berkowicz *et al.* (1996). Similarly, Leitl *et al.* (2001) studied the influence of wind tunnel model detail on pollutant dispersion in street canyons and found notable differences with different degrees of complexity of the model. Other research has clearly shown that the observed changes in flow pattern depended on both geometry and the interaction of different street canyons, for example at street intersections or T-junctions (Scaperdas, 2000). Extensive sets of wind tunnel measurement data around street intersections and buildings is available to researchers on the internet (MIHU, 2001). Wind tunnel studies of the flows in canyons with unequal wall heights have also been conducted (Dabberdt and Hoydysh, 1991). It was found that for a step-up canyon the vortex was significantly stronger than with a symmetrical canyon. In the step-down canyon the measured concentrations were slightly lower on the upwind side. This agrees with numerical simulations (Assimakopoulos *et al.*, 2000), where the highest concentrations seemed to be trapped near the windward-wall.

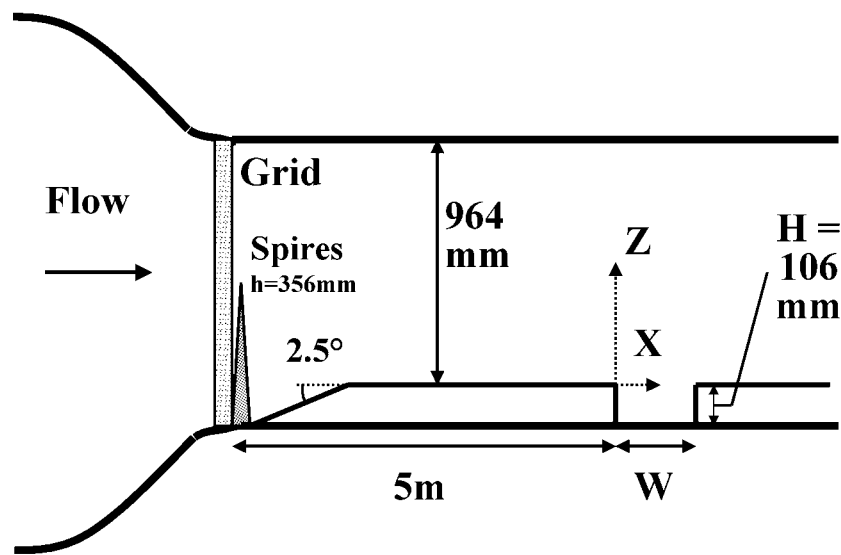


Figure 1. Diagrammatic layout of the wind tunnel and canyon model.

The flows associated with different canyon aspect ratios have been classified by Oke (1987). Since the main canyon vortex directly affects the local distribution of pollutants, the manner in which the flow and the associated turbulence quantities are dependent on the variation of canyon aspect ratio is of key importance. The present research was a study of the mean flow behaviour inside relatively narrow canyons to determine where transitions between different regimes occur. A nominally 2-D street canyon model was exposed to a flow normal to its principal axis and the aspect ratio systematically varied from  $W/H = 0.3$  to  $2.0$ . Detailed profiles of the three wind velocity components were obtained. Parallel to these experiments, the same regimes were numerically simulated with the standard  $k-\varepsilon$  model CHENSI (Sini *et al.*, 1996), run in 2-D to provide mean velocities and turbulent kinetic energy (TKE) for the streamwise (X) and vertical (Z) wind components. For these comparisons, the boundary layer mean velocity and turbulence profiles were used at the inlet of the calculated domain.

## 2. Details of Wind Tunnel Experiments

### 2.1. EXPERIMENTAL ARRANGEMENT

A nominally 2-D cavity of fixed depth ( $H = 106$  mm) was mounted on the wall of a University of Surrey wind tunnel, with its principal axis normal to the wind direction, as shown in Figure 1. The working section dimensions are  $1.37$  m height  $\times$   $1.07$  m width  $\times$   $9$  m length, giving a canyon lateral aspect ratio of  $L/H = 12.9$ .

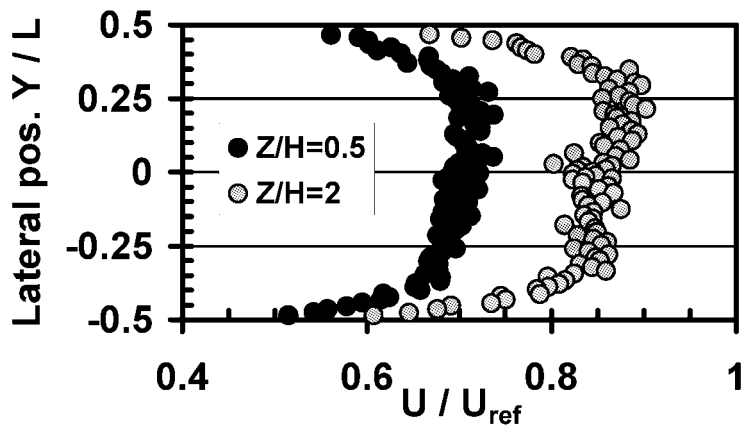


Figure 2. Lateral profiles of  $U$  component mean velocity in the boundary layer.

The streamwise cavity width ( $W$ ) was varied to give 5 cases of  $W/H = 0.3, 0.5, 0.7, 1.0$  and  $2.0$ . A thick turbulent boundary layer was produced by a grid, a fence and vorticity generators at the entrance to the working section, whilst the ground plane and cavity walls were roughened using ‘Lego’ boards with distributed  $4.5 \times 7.5 \times 15$  mm rectangular brick elements. The neutrally stratified approach conditions were; boundary layer height  $\delta = 737$  mm ( $\delta/H = 6.95$ ), roughness length  $z_0 = 0.3$  mm, displacement height  $d = 1$  mm and friction velocity  $U_*/U_{ref} = 0.050$ , based on the freestream velocity  $U_{ref} = 8$  m s $^{-1}$ . The freestream turbulence level,  $u'/U_{ref}$ , was 9% (at  $Z/H = 7$ ), whilst the integral turbulence length scales were typically  $2 H$ ,  $1.5 H$  and  $1.0 H$ , in the X, Y and Z directions, respectively. The test Reynolds number ( $Re$ ) was  $5.6 \times 10^4$ . The flow measurements were taken by pulsed-wire-anemometry, which simultaneously measures the flow speed and direction (Castro and Cheun, 1982). The sampling rate was 50 Hz and 10 000 samples were taken at each point. The measurement data were accurate to within  $\pm 10\%$  for the mean values and  $\pm 15\%$  for the stresses (Castro and Cheun, 1982).

The geometrical scaling of the simulated boundary layer is approximately 1:500, representing an unrealistic 53 m deep full-scale canyon. The resulting roughness length of 0.15 m is certainly not representative of an array of buildings of this height according to the literature (Theurer, 1994). The cavity depth fits a scale of 1:200, giving a building height of approximately 20 m and a scale factor mismatch of 2.5. It is known (Jensen, 1958), that  $H/z_o$  is a key scaling parameter for modelling full-scale cases as too large a scale exposes the model to only small-scale turbulence (Hunt, 1981). However, a mismatch of 2–3 in scaling is acceptable for the present generic study.

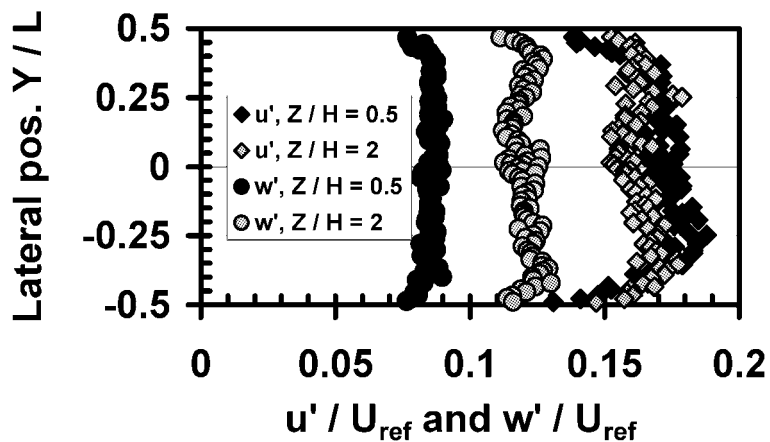


Figure 3. Lateral profiles of  $u'$  and  $w'$  turbulence intensity in the boundary layer.

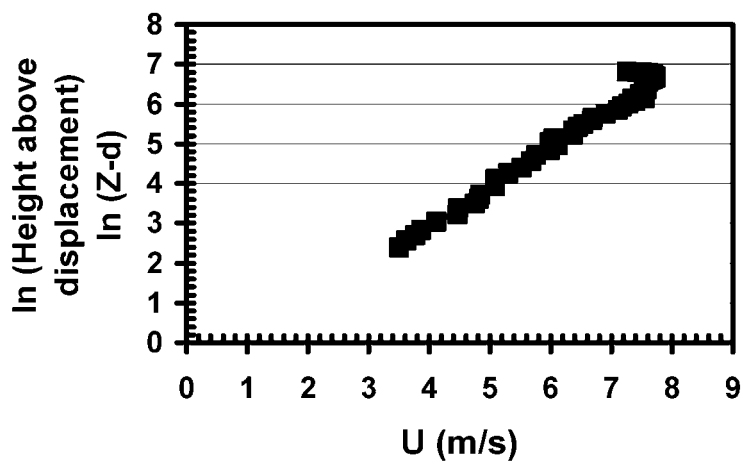


Figure 4. Boundary layer mean velocity profile before separation at cavity.

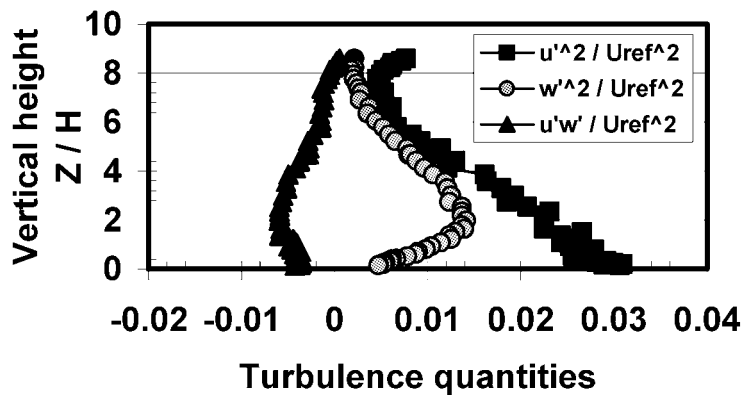


Figure 5. Boundary layer turbulence intensity profiles before separation at cavity.

## 2.2. APPROACH FLOW CONDITIONS

The lateral two-dimensionality in the approach flow and in the cavity was studied extensively to ensure good quality data for CFD validation purposes. This was examined at two heights upstream of the cavity where the boundary layer was already fully developed. The results show that the variation laterally across the boundary layer ( $Y/L$ ) of the  $U$  component mean velocity is consistent to within  $\pm 6\%$  for both heights, Figure 2, whilst the corresponding variations of the  $u'$  and  $w'$  turbulence intensities are within  $\pm 8$  and  $6\%$ , respectively, of the mean value, averaged across the cavity span, Figure 3. Two-dimensionality was clearly established for the central 60% of the spanwise length of the cavity (that is, approximately 7.8 H). The study included some spanwise traverses within the  $W/H = 1.0$  cavity which showed that the  $U$  component was within  $\pm 5\%$  of the mean along each profile. The angle of deviation of the flow direction from the XZ plane (zero for an ideal 2-D flow), was in always less than  $3^\circ$ . The  $u'$  turbulence intensity was within  $\pm 3\%$  of the mean value along each profile. Hence, it may be concluded that the initial conditions were satisfactory for minimising the three-dimensionality effects. The mean velocity and turbulence profiles for the boundary layer, just before separation at the cavity, are shown in Figures 4 and 5, respectively. The small perturbations in the profiles at their outer edges are due to the boundary layer on the opposing side of the tunnel from the canyon model.

## 3. Details of the Numerical Simulations

The numerical simulations used the 3-D CFD code CHENSI (Sini *et al.*, 1996), which is based on the standard  $k-\varepsilon$  model. The turbulent kinetic energy  $k$  and its dissipation rate  $\varepsilon$  are calculated from the semi-empirical transport equations of Hanjàlic and Launder (1972) and the empirical modelling constants are given the most commonly used values for industrial flows (Launder and Spalding, 1974). CHENSI is based on the widely adopted ‘Marker And Cell’ (MAC) method (Hirt *et al.*, 1975), that uses a staggered grid and the solution of a Poisson equation for the pressure at every time-step. The method was initially developed for unsteady problems involving free surfaces; to allow the surface location to be determined as a function of time, markers (massless particles) were introduced into the flow. In CHENSI the method derived from the MAC approach has no markers, but the original staggered grid is retained (scalars located at the mesh centre and velocity components at the centre of the mesh faces). The iterative method for solving the pressure-velocity coupling is also kept. A finite volume method is applied on a non-uniform staggered grid and the three velocity components are defined at the centres of the cell faces while all other scalar dependent variables are located at the cell centres. The numerical procedure uses centred differences for the diffusion and source terms and an upwind-weighted scheme for the advection terms. At

each time step, the continuity condition on mean velocities is directly satisfied by means of the artificial compressibility method described by Chorin (1967). This implicit iterative method simultaneously relaxes velocity and pressure fields in such a way that the Navier-Stokes solution complies with the continuity equation. The numerical procedure is explicit in time. The time-dependent problems are run from the pre-set initial state until steady state conditions are reached. Initial field values within the computation domain are chosen to hasten convergence. In the present case the initial wind speed and TKE field are derived from the experimental boundary conditions. The inlet logarithmic wind profiles are based on the measured  $z_o$  and  $U_*$  values, whilst the turbulence profiles of  $k$  and  $\varepsilon$  are built from measured values, with  $k = (u'^2 + 2w'^2)$ . The boundary conditions are specified in ‘fictive’ cells that border the computation domain. These facilitate the formulation of the boundary conditions and are artifacts for numerical convenience. The flow field is solved in the fluid (real) domain which ‘sees’ the boundary conditions as being the enveloping layer of fictive cells representing the external, uncalculated flow. The von Neumann zero normal derivative condition is used at the top and outflow free boundaries, whilst the near wall region is described by the wall function of Launder and Spalding (1974). The initial experimental conditions, together with the W/H = 2.0 data set, have recently been a test case for numerical model intercomparison within several European institutions (Sahm *et al.*, 2002). This showed that CHENSI predicted the mean flow field to an accuracy as good as the other models.

#### 4. Results and Discussion

##### 4.1. MEAN PROFILES

The results presented here concern the mean flow patterns within the different canyons. Figure 6 shows the comparison between the experiments (symbols) and the CHENSI predictions (lines) of the  $U$  component mean velocity on five vertical profiles within the W/H = 1 cavity. A similar plot for the W/H = 2 case may be found in the paper of Sahm *et al.* (2002). The data sets collapse extremely well within the shear layer above the canyon, with the most upstream profile ( $X/W = 0.09$ ) well predicted immediately below the shear layer. Through the cavity the agreement is good, although CHENSI tends to underpredict the magnitude of the positive and reversed flow velocities, as noted by Sahm *et al.* (2002). The discrepancy is greatest near the cavity base, probably due to the wall function used in the model. However, in regions where the velocity is low (e.g. for W/H = 0.7, not shown here) the CHENSI predictions agree well with the experiment. The differences between the experimental and predicted data near the wall may be significant when modelling traffic pollution. The bottom of the canyon is where traffic emissions take place and so correct modelling of the flow in this region may be of crucial importance in some canyon flow and dispersion scenarios.

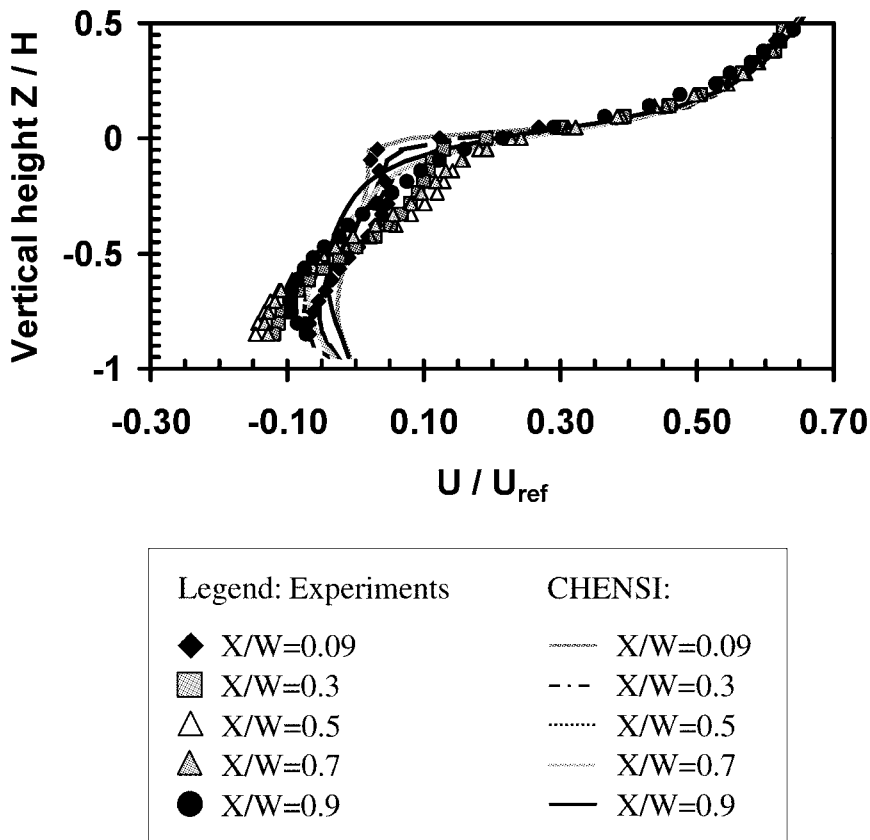


Figure 6. Comparison of  $U$  component velocity distributions in canyon,  $W/H = 1$ .

#### 4.2. SKIMMING FLOW

Projected mean velocity vectors on the XZ centre-plane ( $Y = 0$ ) for all the 5 cases, together with their streamtrace patterns, are shown in Figures 7 to 11. Each figure shows the experimental data plot followed by the CHENSI predictions. All the cases studied show the skimming flow regime, with the separating shear layer originating from the upstream cavity corner passing across the cavity opening with little deflection into the canyon. This agrees with Johnson and Hunter's (1999) field observations of a skimming flow regime up to an aspect ratio threshold of  $W/H = 2.5$ . Earlier numerical simulations gave a threshold value of  $W/H = 1.54$  (Hunter *et al.*, 1992; Sini *et al.*, 1996).

#### 4.3. VORTEX STRUCTURE

Both predictions and measurements show a dominant vortex within the canyon for  $W/H = 2.0$  and 1.0, but only the  $W/H = 2.0$  case also shows a clear secondary

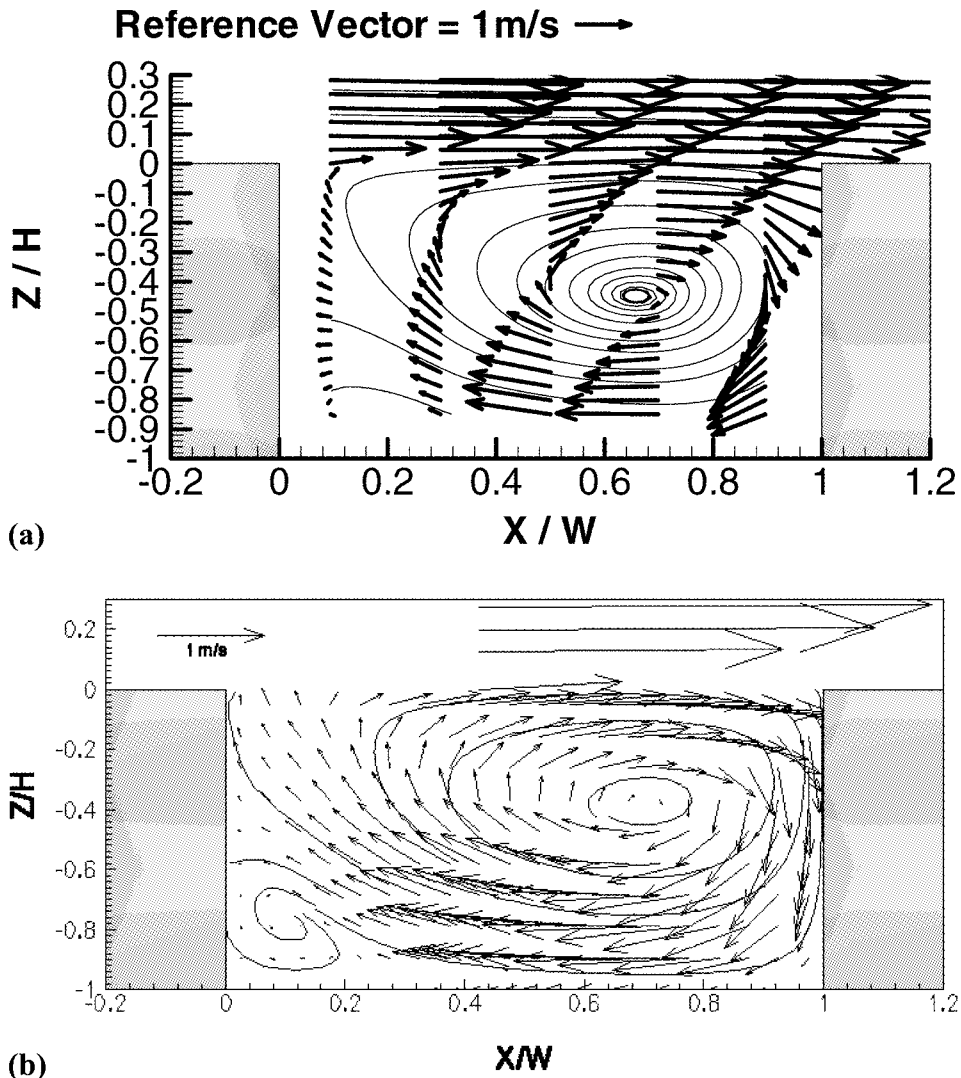


Figure 7. Mean velocity vectors and streamtraces on centre-plane for  $W/H = 2.0$ . (a) Experiments, (b) CHENSI.

vortex near the upstream wall. For a reduced aspect ratio,  $W/H = 0.7$ , the main vortex remains, but a recirculation region appears near the ground next to the *downstream* wall in both the experiments and predictions. In the  $W/H = 0.5$  case the lower of these two vortices grows in size, although it remains considerably weaker than the upper recirculation. In the experiments the centre of the secondary vortex remains close to the downstream wall whereas the predictions show a more centred vortex. The same features, but less pronounced, are found for  $W/H = 0.3$ , where the experiments show almost zero velocity in the lowest third of the cavity, indicating

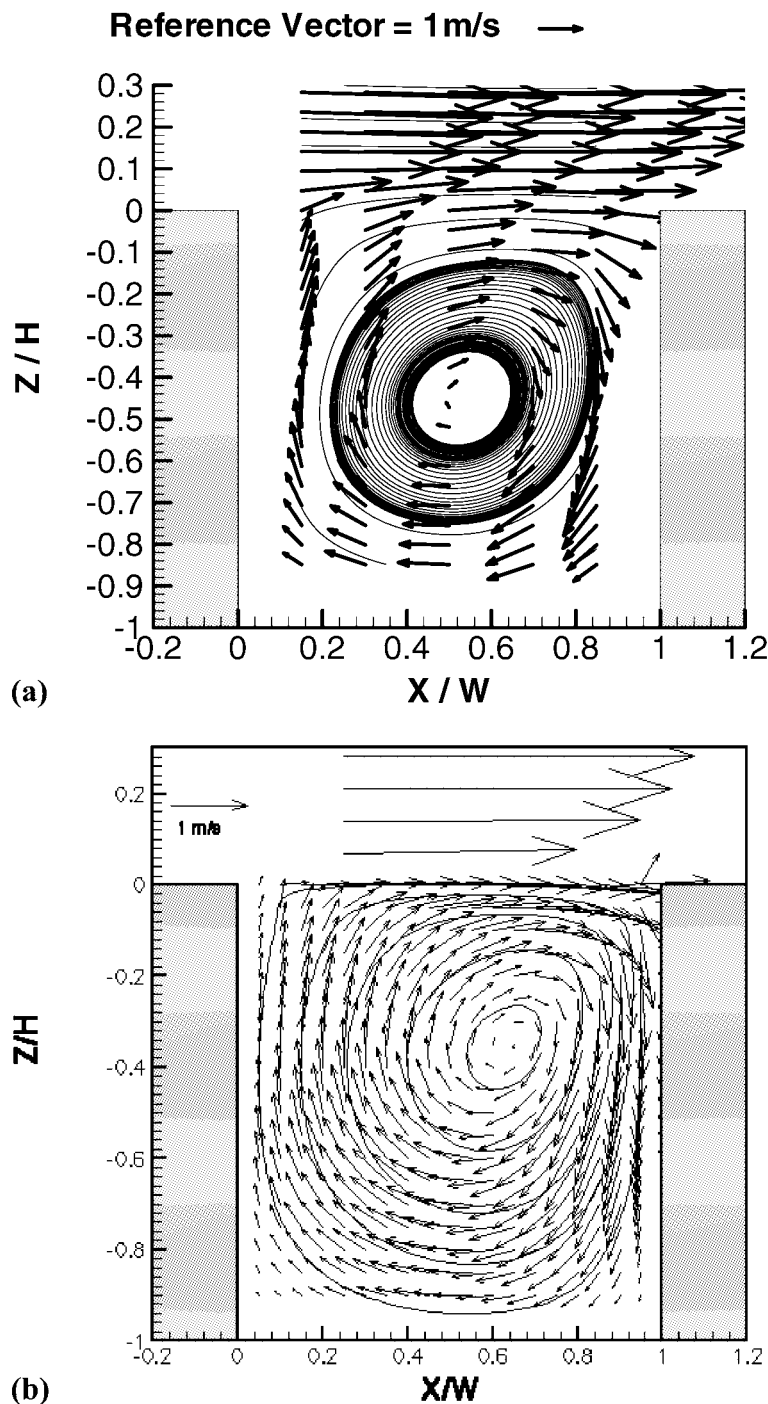


Figure 8. Mean velocity vectors and streamtraces on centre-plane for  $W/H = 1.0$ . (a) Experiments, (b) CHENSI.

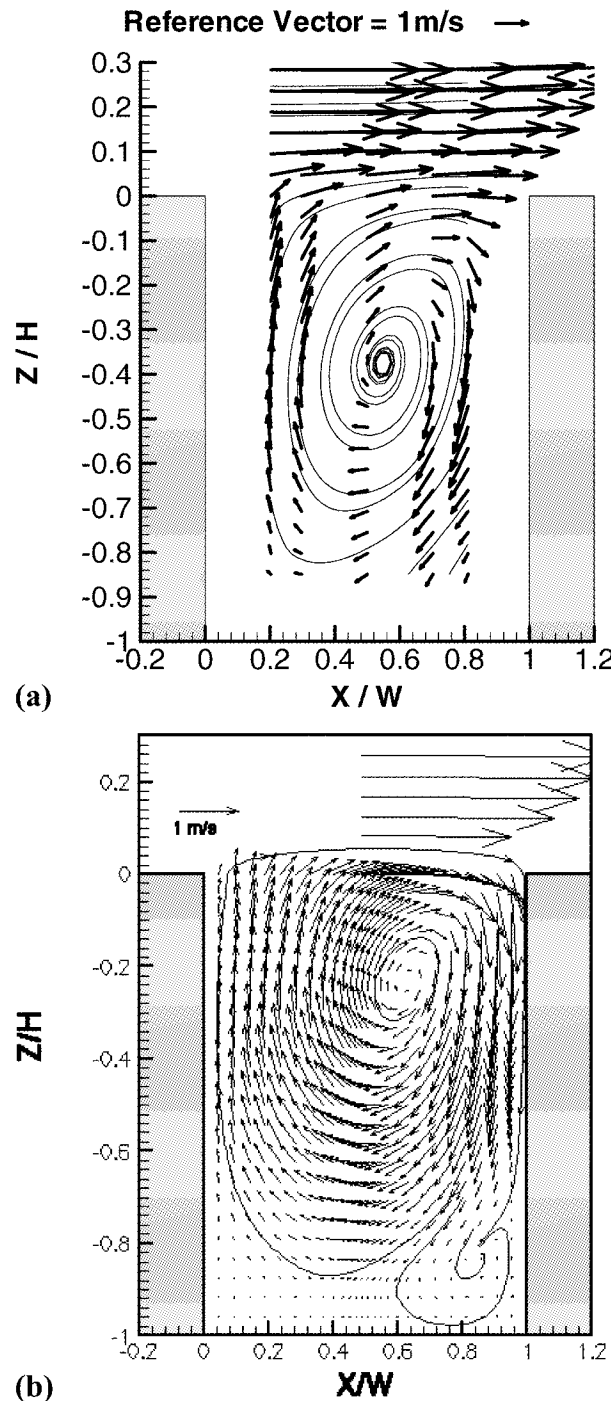


Figure 9. Mean velocity vectors and streamtraces on centre-plane for  $W/H = 0.7$ . (a) Experiments, (b) CHENSI.

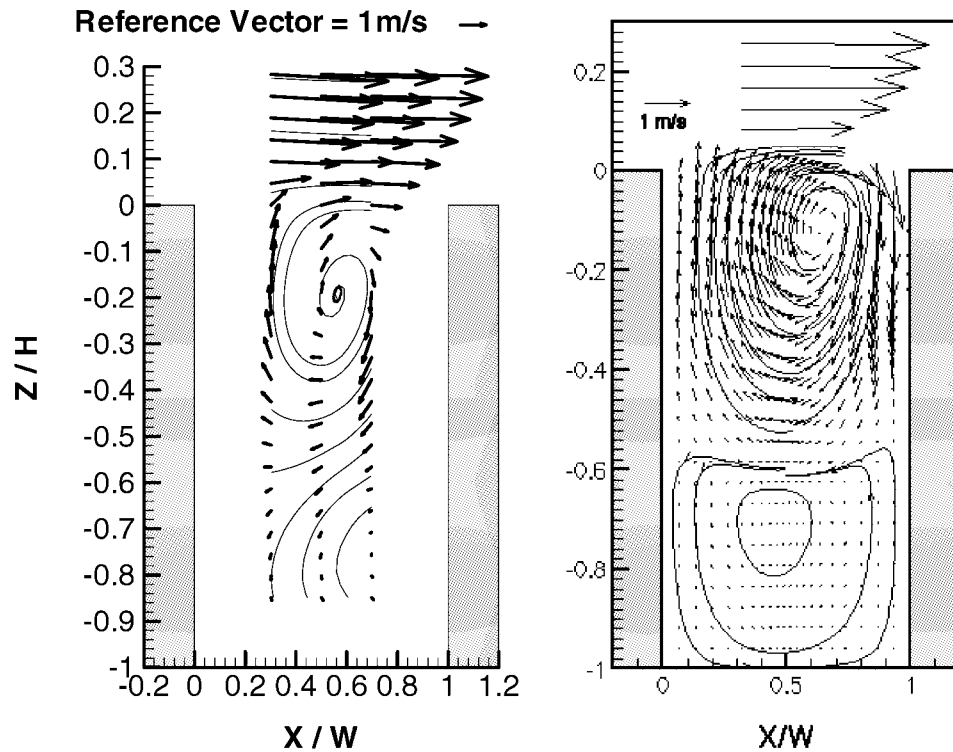


Figure 10. Mean velocity vectors and streamtraces on centre-plane for  $W/H = 0.5$ . (a) Experiments, (b) CHENSI.

a flow weakly connected to that above, giving very poor ventilation properties. The numerical predictions show 3 vortices immediately above each other, with the lowest vortex being the weakest of them.

The centre of the upper vortex in the simulations is always closer to the downstream wall and higher within the canyon when compared to the experiments. This is shown in Figure 12 by coordinates of the vortex centre ( $X_c, Z_c$ ) presented as a plot of experiments versus predictions. The predictions are always 5–15% greater than the experimental values, indicating a tighter vortex in the upper downstream part of the cavity, perhaps due to a weaker diffusion of vorticity in the predictions. Whilst the height of the vortex centre increases with decreasing  $W/H$ , its downstream location remains static for  $W/H \leq 1$ , at about  $X_c/W = 0.55$  and 0.65 for the experiments and predictions, respectively.

It is known that the flow in regularly shaped canyons is strongly influenced by initial conditions, with the boundary layer friction velocity being a suitable normalising parameter for some aspects of the flow, such as wall pressure distributions and overall cavity drag force. Other recent work (Kovar-Panskus *et al.*, 2002), in which a different canyon with  $W/H = 1$  was subjected to a boundary layer with  $U_*/U_{ref}$

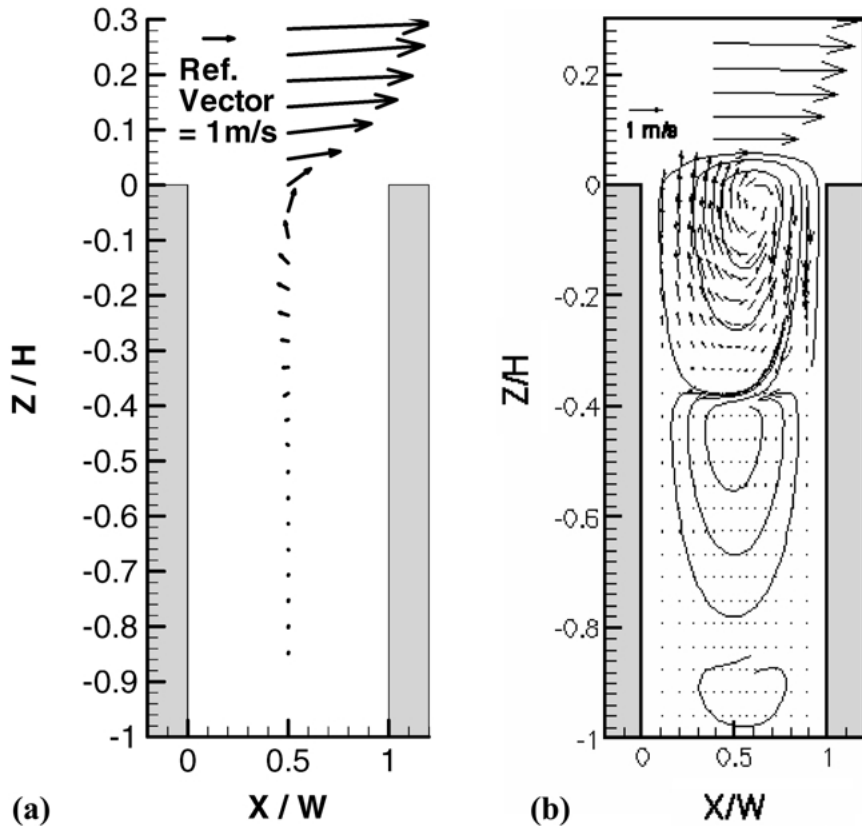


Figure 11. Mean velocity vectors and streamtraces on centre-plane for  $W/H = 0.3$ . (a) Experiments, (b) CHENSI.

$= 0.070$ , gave a maximum reversed flow velocity near the ground of  $0.19 U_{ref}$ . This is greater than the  $0.15 U_{ref}$  obtained here for a lower friction velocity of  $U_*/U_{ref} = 0.050$ , indicating the role of the skin friction in driving the canyon flow. This second study gave a vortex centre location of  $X_c/W = 0.64$ ,  $Z_c/H = -0.50$ , compared to 0.53 and  $-0.44$ , respectively, in the present study, again showing the sensitivity of the flow pattern to initial conditions.

## 5. Concluding Remarks

A wind tunnel investigation and a numerical study using the CFD code CHENSI have been conducted to investigate the flow regimes within a nominally 2-D cavity with  $W/H$  varied from 0.3 to 2.0. For all the cases under consideration the skimming flow regime has been observed, indicating that the transition to wake interference flow takes place at an aspect ratio of  $W/H > 2.0$ . The agreement between the wind tunnel measurements and the numerical study, using the same inlet bound-

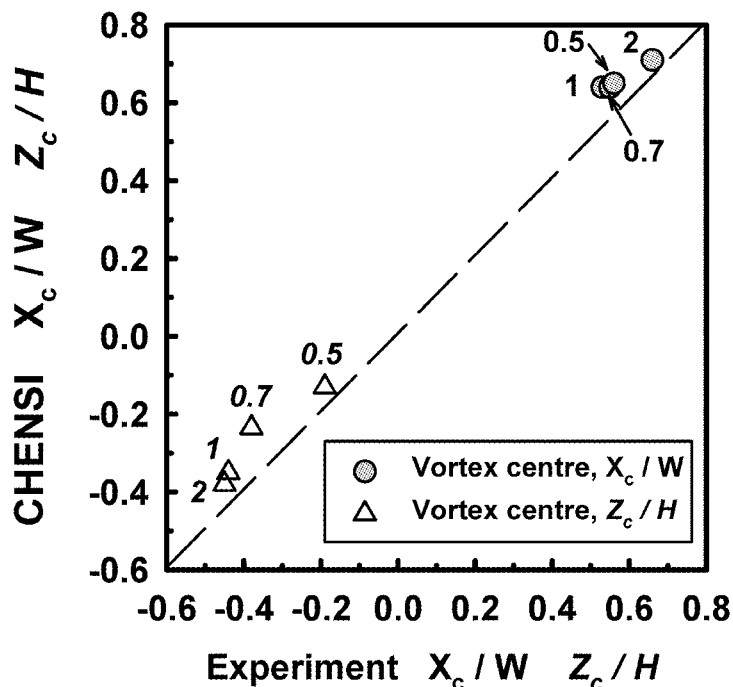


Figure 12. Comparison of the experimental and predicted location of the primary vortex centre ( $X_c$ ,  $Z_c$ ). Data points labelled by  $W/H$ ,  $Z_c$  location in *italics*.

ary conditions was reasonably good, although CHENSI tended to underpredict the magnitudes of the velocities within the canyon. The main flow features, in terms of the large vortex structures, were predicted extremely well. However, the centre of the main vortex was 5–15% higher and more downstream in the cavity in the predictions than in the experiments, indicating a tighter and less diffuse vortex. Further work is required to clarify the influence of initial conditions on the flow regimes in canyon configurations and to achieve a suitable parameterisation of those conditions.

#### Acknowledgements

Thanks are due to the EU (TRAPOS project funding), Mr. T. Renouf and the Institut de Développement et de Recherche pour l'Informatique Scientifique (IDRIS), France.

## References

- Assimakopoulos, V., ApSimon, H., Sahm, P. and Moussiopoulos, N.: 2000, 'Effects of Street Canyon Geometry on the Dispersion Characteristics in Urban Areas', *Proceedings of the 16th IMACS World Congress*, 21–25 August 2000, Lausanne, Switzerland.
- Berkowicz, R., Hertel, O., Larsen, S. E., Sorensen, N. N. and Nielsen, M.: 1997, *Modelling Traffic Pollution in Streets*, NERI, Roskilde, Denmark.
- Castro, I. P. and Cheun, B. S.: 1982, 'The measurement of Reynolds stresses with a pulsed-wire anemometer', *J. Fluid Mech.* **118**, 41–58.
- Dabberdt, W. F. and Hoydysh, W. G.: 1991, 'Street canyon dispersion: Sensitivity to block shape and entrainment', *Atmosph. Environ.* **25A**, 1143–1153.
- DePaul, F. T. and Sheih, C. M.: 1986, 'Measurements of wind velocities in a street canyon', *Atmosph. Environ.* **20**, 555–559.
- Hanjàlic, R. and Launder, B. E.: 1972, 'A Reynolds stress model of turbulence and its application to thin shear flows', *J. Fluid Mech.* **52**, 609–638.
- Hirt, C. W., Nichols, B. D. and Romero, N. C.: 1975, 'Sola: A Numerical Solution for Transient Fluid Flows', *Report LA5852*, Los Alamos Laboratory, University of California, Los Alamos Scientific Laboratory, New Mexico 87544, U.S.A.
- Hunt, A.: 1981, 'Scale Effects on Wind Tunnel Measurements of Surface Pressures on Model Buildings', *Proceedings of Colloquium 'Designing with the Wind'*, CSTB, Nantes, France.
- Hunter, L. J., Johnson, G. T. and Watson, I. D.: 1992, 'An investigation of three-dimensional characteristics of flow regimes within the urban canyon', *Atmosph. Environ.* **26B**, 425–432.
- Jensen, M.: 1958, 'The model law phenomena in natural wind', *Ingenioren* **2**, 4.
- Johnson, G. T. and Hunter, L. J.: 1999, 'Some insights into typical urban canyon airflows', *Atmosph. Environ.* **33**, 3991–3999.
- Kastner-Klein, P. and Plate, E.J.: 1999, 'Wind tunnel study of concentration fields in street canyon', *Atmosph. Environ.* **33**, 3973–3979.
- Kovar-Panskus, A., Moulinneuf, L., Savory, E., Abdelqari, A., Sini, J.-F., Rosant, J.-M., Robins, A. and Toy, N.: 2002, 'A wind tunnel investigation of the influence of solar-induced wall-heating on the flow regime within a simulated urban street canyon', *Water, Air, and Soil Pollut.*, this issue.
- Launder, B. E. and Spalding, D. B.: 1974, 'The numerical computation of turbulent flows', *Comp. Meth. Appl. Mech. Eng.* **3**, 269–289.
- Liedtke, J., Leitl, B. and Schatzmann, M.: 1999, 'Dispersion in a street canyon: comparison of wind tunnel experiments with field measurements', in P. M. Borrel and P. Borrel (eds), *Proc. of Eurotrac Symposium '98*, WIT Press, Southampton, pp. 806–810.
- Leitl, B., Chauvet, C. and Schatzmann, M.: 2001, 'Effects of Geometrical Simplifications and Idealization on the Accuracy of Microscale Dispersion Modelling', *Extended abstract for the 3rd International Conference on Urban Air Quality*, 19–23 March 2001, Loutraki, Greece.
- M.I.H.U.: 2001, Internet database, available at University of Hamburg, funded by the Umweltbundesamt: <http://www.mi.uni-hamburg.de/cedval/categoryB.htm#B1-5>.
- Nakamura, Y. and Oke, T. R.: 1988, 'Wind, temperature and stability conditions in an E–W-oriented canyon', *Atmosph. Environ.* **22**, 2691–2700.
- Oke, T. R.: 1987, *Boundary Layer Climates*, 2nd ed., Routledge, New York.
- Pavageau, M., Rafailidis, S. and Schatzmann, M.: 1996, 'A Comprehensive Experimental Databank for the Verification of Urban Car Emission Dispersion Models', *Proceedings of the 4th Workshop on Harmonisation within Atmospheric Dispersion Modelling for Regulatory Purposes*, 6–9 May 1996, Ostende.
- Rafailidis, S.: 1997, 'Influence of building area density and roof shape on the wind characteristics above a town', *Bound. Layer Meteor.* **85**, 255–271.

- Sahm, P., Louka, P., Ketzel, M., Guilloteau E. and Sini, J. F.: 2002, 'Intercomparison of numerical urban dispersion models - Part I: Street canyon and single building configurations', *Water, Air and Soil Pollut.*, this issue.
- Scaperdas, A.: 2000, 'Modelling Air Flow and Pollutant Dispersion at Urban Canyon Intersections', Ph.D. Thesis, University of London.
- Sini, J.-F., Anquetin, S. and Mestayer, P.: 1996, 'Pollutant dispersion and thermal effects in urban street canyons', *Atmosph. Environ.* **30**, 2659–2677.
- Theurer, W.: 1994, 'Ausbreitung bodennaher Emissionen in komplexen Bebauungen', *Mitteilungen, Heft 45*, Institut für Hydrologie und Wasserwirtschaft, Universität Karlsruhe, Germany.